

Article

Recent Applications of Unilateral NMR to Objects of Cultural Heritage

Valeria Di Tullio  and Noemi Proietti * 

Institute of Heritage Science (ISPC), CNR, Area della Ricerca di Roma 1, Via Salaria Km 29,300, 00015 Moterotondo, Roma, Italy; valeria.ditullio@cnr.it

* Correspondence: noemi.proietti@cnr.it

Abstract: Although nuclear magnetic resonance (NMR) is recognized as a powerful tool in many areas of research, among the investigative techniques used in the field of cultural heritage its application is still largely unknown. One of the reasons for this is that artifacts are complex heterogeneous systems whose analysis requires a multi-disciplinary approach. In addition, major drawbacks in the analysis of objects belonging to cultural heritage are their limited quantity, number of samples collected from the artifact, and their immovability. Consequently, a methodological approach where non-destructive, and possibly non-invasive techniques are used, is advisable. In recent years, thanks to the development of portable instruments, there has been an increasing use of the NMR methodology in the cultural heritage field. The use of portable NMR has allowed us to study several materials in the cultural heritage, such as frescoes, stones, wood, paper, and paintings, to address the challenges in monitoring dampness in historical masonries, to evaluate the penetration depth of a hydrophobic treatment into a porous material, and to study of the effect of cleaning procedures on artifacts. In this paper, recent studies illustrating the potential of NMR portable methodologies in this field of research are reported.

Keywords: portable NMR; cultural heritage; monitoring; degradation; treatments; NMR stratigraphy



Citation: Di Tullio, V.; Proietti, N. Recent Applications of Unilateral NMR to Objects of Cultural Heritage. *Heritage* **2024**, *7*, 2277–2295. <https://doi.org/10.3390/heritage7050108>

Academic Editors: Silvano Mignardi, Wenke Zhao, Laura Medeghini, Melania Di Fazio and Laura Calzolari

Received: 9 March 2024

Revised: 23 April 2024

Accepted: 23 April 2024

Published: 29 April 2024



Copyright: © 2024 by the authors. Licensee MDPI, Basel, Switzerland. This article is an open access article distributed under the terms and conditions of the Creative Commons Attribution (CC BY) license (<https://creativecommons.org/licenses/by/4.0/>).

1. Introduction

The study of the state of conservation of cultural heritage and its monitoring over time represents a complex field. Many works of art show different challenges, including the necessity to minimize both the quantity and the number of samples collected from artifacts. Moreover, often the objects to be analyzed are immovable and cannot be brought to the laboratory for analysis. Over the past twenty years, research has sought to address these issues by developing progressively advanced technologies that are mostly portable and non-invasive [1,2]. Decades of technological advances in instrumental analysis have transformed numerous techniques from laboratory innovations into portable non-invasive analytical tools with increasing applicability to the study of cultural heritage objects. The magnetic resonance technique is among these technologies. Despite being developed in the 1950s, its application to cultural heritage is relatively recent. This is largely due to the fact that NMR spectrometers are typically large, expensive, and immovable, making them less commonly available in many laboratories. Furthermore, even with the development of new methodologies aimed at reducing the quantity of required samples [fast-MAS NMR], there is still a demand for a substantial amount of samples (mg) for analysis. The development of portable unilateral NMR sensors in the 2000s [3–8] marked an advancement in the application of magnetic resonance to cultural heritage collections [9–12]. This technique is increasingly employed to investigate the state of conservation and degradation of works of art, as well as to monitor the effectiveness of treatments applied to materials within the realm of cultural heritage [13–16].

In portable NMR sensors, in which the object is taken close to the stray magnetic field, the magnet geometry is referred to as an open geometry. In this configuration,

the magnet is placed to one side of the object, fully preserving the integrity and the dimension of the sample under investigation, while also facilitating measurements of precious materials. Because of this peculiarity, portable NMR sensors are also called unilateral NMR or single sided NMR sensors. A drawback of these types of sensors is the inhomogeneity of the magnetic field, which limits the type of experiments that can be carried out. Due to the inhomogeneous magnetic field, the signal (FID) decays rapidly and cannot be directly detected, as performed with benchtop and laboratory NMR spectrometers. Therefore in portable NMR sensors, the signal must be recovered as an echo allowing for the measurements of NMR parameters such as proton density, longitudinal T_1 and transverse T_2 relaxation times, self-diffusion coefficient, and even the collection of 2D T_1 – T_2 Maps [17]. The decay of magnetization in the xy plane is frequently dominated by the field inhomogeneity effect, and the transverse relaxation time is generally referred to as T_2^* , which is always shorter than that measured in a homogeneous field. T_2^* is used to explain such observed decay, as it considers both the natural T_2 relaxation (spin–spin interaction) and the relaxation due to magnetic field inhomogeneity (T_2'), as described in Equation (1):

$$\frac{1}{T_2^*} = \frac{1}{T_2} + \frac{1}{T_2'} \quad (1)$$

In Figure 1 are illustrated two typologies of portable unilateral NMR sensors: Figure 1a shows a palm-sized NMR sensor. It consists of a U-shaped magnet obtained using two anti-parallel permanent magnets mounted on an iron yoke with the rf coil positioned in the gap of the magnet. The magnetic field is external to the device, enabling large objects to be studied without any sampling. Different probe heads, each tuned to the proper frequency are used to obtain different depths of measurement. Changing the radiofrequency inside the iron yoke, it is possible to range the penetration depth of 0 mm, 3 mm, and 5 mm, corresponding to a sensitive volume of $1 \times 20 \times 50 \text{ mm}^3$.

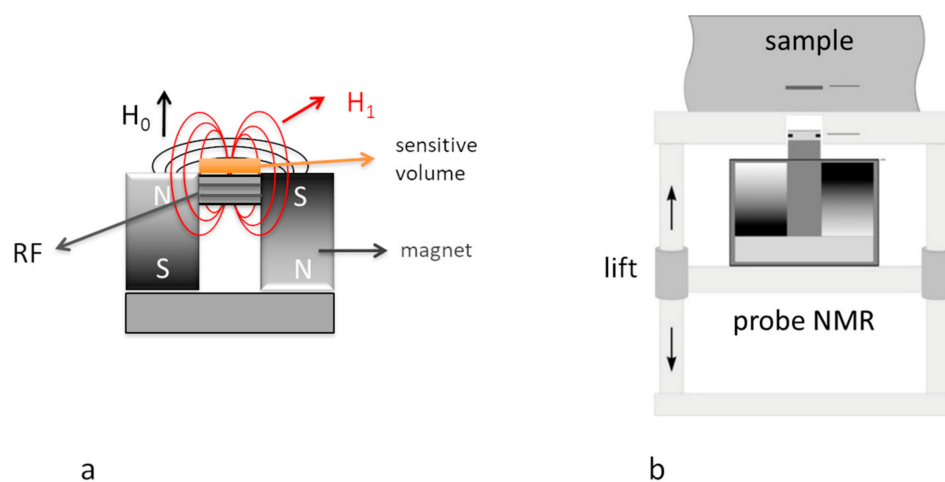


Figure 1. (a) U-shaped unilateral NMR sensor by Bruker Biospin; (b) unilateral NMR sensor by Magritek. The sensor is placed on a lift that allows one to move the magnetic field inside the object to be analyzed with micrometric steps.

Figure 1b shows a further development of unilateral NMR sensors by Magritek that can scan depths from 0 up to 1.0 cm. This sensor generates a magnetic field with an exceptional extremely uniform gradient, enabling the resolution of near-surface structures in arbitrarily large samples. To improve gradient uniformity, the device works at a fixed depth from the sensor, where high depth resolution can be achieved. The position of the excited slice inside the sample can be varied by displacing the sensor using a high-precision lift that repositions the magnet with respect to the sample, producing depth profiles with micrometric spatial resolution [5,8]. These devices have opened further possibilities of application in the field of cultural heritage [15,16,18].

2. Results and Discussion

2.1. Monitoring Moisture in Masonry

The presence of water in historic masonry is one of the most pressing conservation problems for architectural heritage [19,20] and, more generally, ancient buildings. The moisture presence can be attributed to several origins: accidental causes (roof infiltration, pipe leaks, etc.), condensation (both on the outer surface and inside the masonry), precipitation caused by wind [21,22], hygroscopic salts [23], floods [24] and floods underground, where water is supplied by aquifers under clay soils, underground watercourse [25], and poor drainage of precipitation [26], etc.

The movement of water inside building materials acts as a carrier for the salt contents dissolved in solution, transporting them from the inside of the masonry to the surface. Since the salts cannot evaporate, they are deposited inside the pores in correspondence with the evaporation section, both superficial in the case of plaster, and internal in the case of masonry.

The saturation of the porous system, due to the continuous deposit of salts, determines the occurrence of states of stress that produce bulges, detachments, and the phenomena of surface degradation (Figure 2).

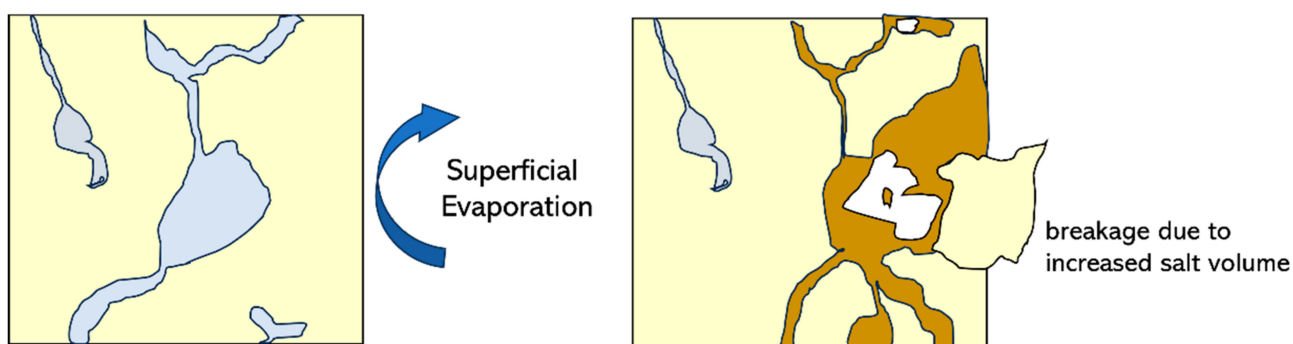


Figure 2. Surface degradation due to deposit of hygroscopic salts.

Knowledge of the water path and its distribution through the wall is mandatory to determine the mechanism by which the water causes and accelerates damage [27], whereas humidity in historic masonry often affects buildings that contain architectural and artistic evidence such as museums, art galleries and noble palaces. An accurate diagnosis of the causes and the extent of humidity is a fundamental step to be performed before the conservation work. Nevertheless, the amount and the distribution of moisture within a wall painting is difficult to determine. The methods currently used for this determination are IR thermography (IRT), electrical conductivity, and gravimetric tests. IRT does not allow a quantitative evaluation of the moisture content, electrical conductivity may be affected by the presence of salts, and gravimetric tests are a highly invasive technique, requiring sampling by core drilling, which is strictly forbidden in the case of precious artworks such as wall paintings.

Over recent years, several studies have allowed the validation of portable NMR techniques as an analytical and non-invasive tool for quantitative mapping in situ, in a fully non-invasive way, the moisture distribution in precious and ancient deteriorated masonries and wall paintings [27,28].

By performing a suitable number of NMR measurements on a matrix of points, the NMR data are processed to obtain a contour plot, which is a 2D representation of a 3D surface, where x and y are the coordinates of the measured area of the masonry and z is the integral of the NMR echo signal. The contour plot obtained allowed for an easy visualization of the distribution of the moisture in the wall painting; the difference in the moisture levels are represented as a gradient of color, dark red indicates the lowest moisture content, whereas dark blue indicates the highest moisture content.

The peculiarity of the portable NMR methodology is that the intensity of the signal detected by NMR is directly proportional to the water content [29]. This allows for the calibration of the integral of the recorded signal NMR in order for each area of the map to correspond with an accurate amount of moisture.

In detail, the calibration of the ^1H NMR signal was carried out using 4 model plaster samples prepared to reproduce the same type of mortar used in the wall under investigation. The calibration between the water content of the model samples (Moisture Content (MC)), and the NMR signal was obtained by using the imbibition coefficient (ic), defined as the maximum amount of water adsorbed by the specimen compared to its dry weight, according to the following equations [28]:

$$MC_{(NMR)} = (A_i - A_{min}) \left\{ \frac{ic}{A_{S_w} - A_{S_d}} \right\} \quad (2)$$

$$ic = \frac{(P_{S_w} - P_{S_d})}{P_{S_d}} \quad (3)$$

where A_i is the amplitude of the NMR signal measured on the masonry, A_{min} is the lowest value of the amplitude measured on the masonry, and A_{S_w} and A_{S_d} are the average values of the amplitude of the NMR signal measured in the water-saturated and dried model plaster samples, respectively. P_{sd} and P_{sw} are the weights of the model plaster samples in dried and water-saturated conditions. According to this calibration procedure, each area of the contour plot map corresponds to an accurate amount of moisture.

Different humidity source damage in masonries can be found. In this paper, three typologies will be discussed: moisture due to rising damp, moisture in hypogeous environments, and moisture due to condensation phenomena. These studies on moisture in the masonries are performed by using a U-shaped unilateral NMR sensor, as reported in Figure 1a. Rising damp is one of the most recurrent and well-known hazards to existing buildings and monuments. As the phenomenon of rising damp is quite slow, the damage of the building materials and structures may become visible only after several years from the construction. The mechanism behind the phenomenon of rising damp in a wall is based on capillarity [19,20,30–32]. It is a physical event that exploits the surface tension between a liquid and a solid. Capillary forces drive water from the ground to the wall, defying gravity forces. The rising humidity can reach several meters in height and theoretically can reach up to 15 m. Actually, the level of rising is limited to about one or two meters because it depends on the porosity of the material and the evaporation phenomena. Generally, the damage due to capillary rise afflicts the historic masonries that are in the vicinity of water courses or in wetlands, aggravated by extreme weather phenomena that characterize climate change in progress. The San Nicola in Carcere church in Rome, located near the Tiber River in an area that must have been originally swampy and subject to the floods, is a study case falling within this first category. The high levels of humidity affected the wall of the church for a long time, which made it necessary to periodically remake its wall paintings. The church was the subject of a multidisciplinary study within a regional project ADAMO Project (Analysis, Diagnostic and Monitoring Technologies for the conservation and restoration of cultural heritage) for the presence of important water infiltrations in the apse. A campaign of measures was carried out by a multidisciplinary non-invasive approach for the evaluation of the content and moisture distribution in the lower part of the apse of the church. Unilateral NMR was one of the techniques used for non-invasive analysis [33]. To map the moisture distribution, a probe of 3 mm depth was used.

Figure 3 showed the moisture distribution map obtained in the San Nicola apse by unilateral NMR sensors. The contour plots obtained (Figure 3c) allowed us to visualize the height of the wetter areas of the apse. In particular, the wet front reaches a height of about 1800 on the left and 1500 cm on the right of apse.

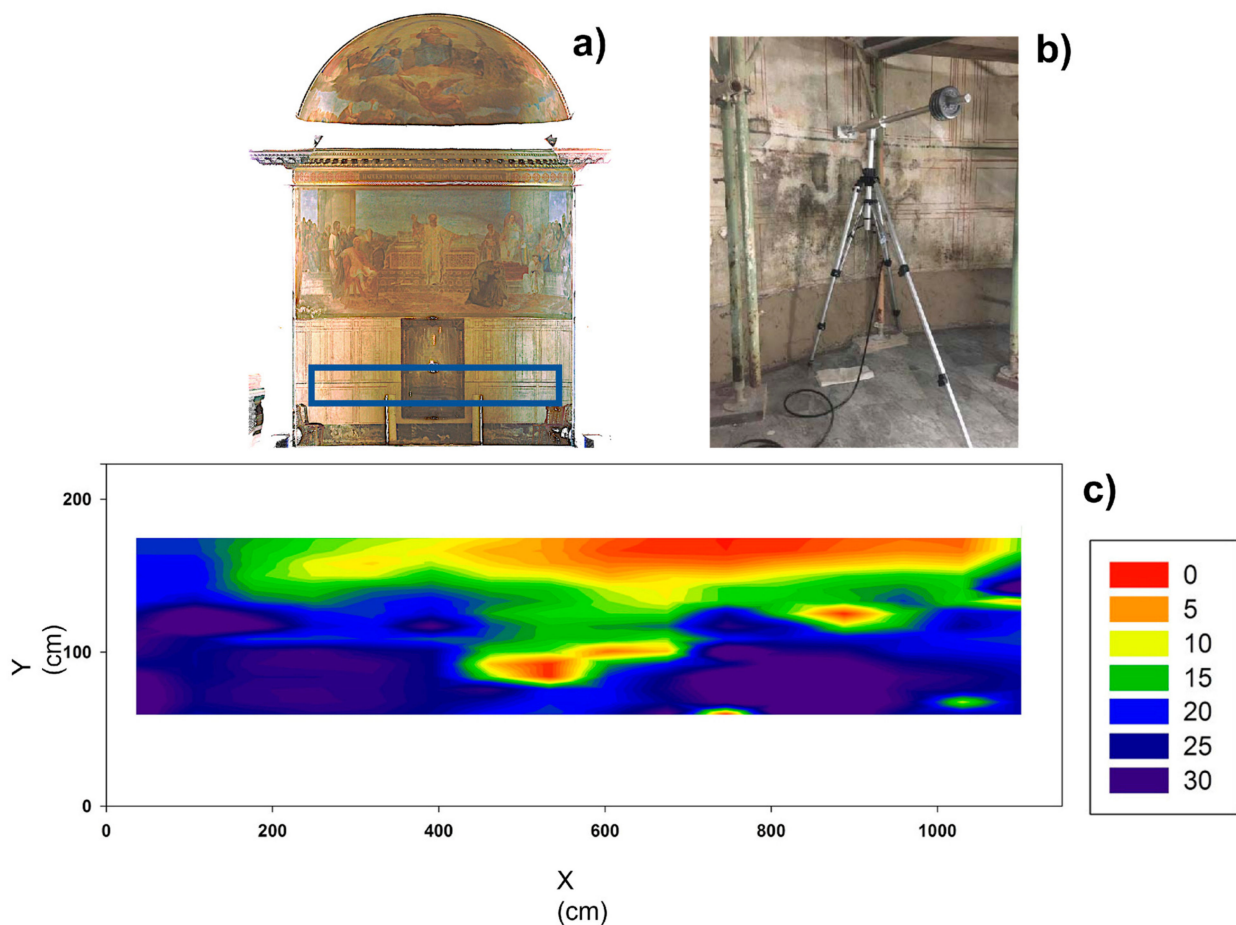


Figure 3. (a) The blue box shows the area of the apse in the church of “San Nicola in Carcere”, analyzed by NMR unilateral sensor; (b) portable NMR during the acquisition; (c) Humidity map recorded by unilateral NMR at the depth of 3 mm of the San Nicola apse. The legend provides the humidity content range (%) obtained by calibrating the NMR signal.

By performing the calibration of the maximum NMR proton signal by model samples described above, in the most humid region a moisture content (MC NMR) value of 30% was found.

Another case of moisture damage is what happens in hypogeal environments. The hypogeal environments are underground environments, or cavities, which can be both natural, such as karst caves, or artificial, such as hypogeal museal environments, i.e., catacombs, and they are characterized by very high relative humidity levels and generally very low temperatures. The conservation of underground environments is a problem with challenging solutions, due to the complex dynamics that characterize the physical–chemical–biological interactions between the hypogeal structure and surrounding environment.

Finally, the hypogeal environments, in addition to being affected by changes in temperature and internal humidity, are continuously subject to the risk of water infiltration, due to rainwater percolation and any underground aquifers present.

The experiences conducted in typical underground environments, such as the Etruscan necropolis and the catacombs, have indicated in the processes of thermo-hygrometric exchange the main causes of the mechanisms of chemical degradation, such as the cycles of salt crystallization, biological degradation, such as the formation of microorganisms and algae.

The approach of using unilateral NMR sensors to map moisture distribution was recently applied to the Greek Chapel in the catacombs of Priscilla, Rome. The catacombs of Priscilla were one of the first cemeteries to be found in the sixteenth century. The Greek

chapel is named due to two Greek inscriptions painted in the right niche. It is richly decorated with paintings and stuccoes in a Pompeian style and it has a particular shape with three niches for sarcophagi. The purpose of the study was to monitor the moisture status of the paintings in the Greek Chapel in two different times of the year: July, summer heat, and March, a rainy spring period. This study was part of the REMEDIA Project “Research and diagnostics of methods to contrast the deterioration caused by humidity in Cultural Heritage”.

In Figure 4b, the moisture distribution maps obtained by unilateral NMR sensors at a depth of 5 mm from the surface are shown. In July 2022, moisture content is confined in the upper part of the masonry with a percentage of about 20–22%, while the lower part of the map shows lower humidity levels, about 8–10%, suggesting a drying process of the masonry in the summer season. In March 2023, the levels of humidity are localized in the center of the masonry, with values between 13 and 23% and higher due to the frequent rains in springtime.

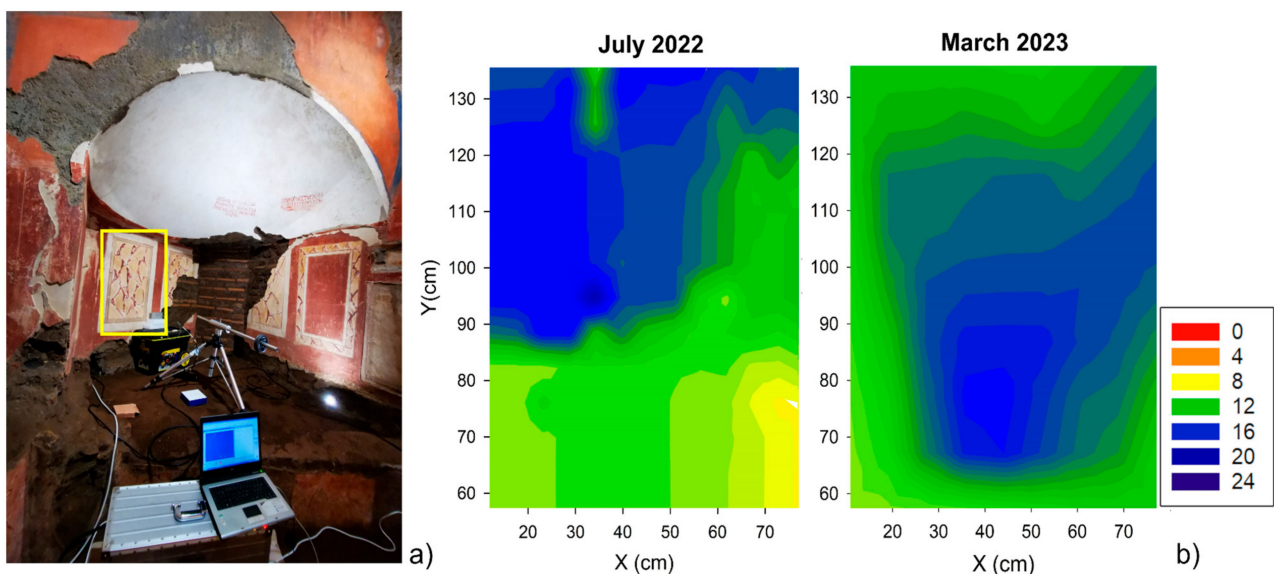


Figure 4. (a) Area (yellow circled) investigated by unilateral NMR sensors in the Greek Chapel, in the Catacombs of Priscilla, Rome; (b) Humidity maps recorded by NMR sensors at a depth of 5 mm from the surface in July 2022 (left) and in March 2023 (right), respectively. The legend provides the humidity content range (%) obtained by calibrating the NMR signal.

The third analyzed case of damage due to moisture is the condensation of air moisture on the masonry. Condensation can occur both on the outer surface of the walls and inside the porous masonry structure. Surface condensation occurs when the air vapor is in contact with a cold, condensed surface; this is because in some places or in some areas of the wall the internal surface temperature is lower than the so-called “dew temperature”, which means the temperature below the steam condenses. Interstitial condensation relates to the diffusion of steam through the walls that divide rooms at different temperatures and at relative humidities, and occurs at the inner layers of masonry when a correct sequence of layers is not realized.

In these processes, temperature fluctuations play a significant role, leading to the accumulation of moisture on surfaces and, in some cases, affecting the deeper layers of the masonries.

In addition, the presence of hygroscopic salts further aggravates the damage. These salts in fact could absorb moisture from their surroundings, becoming a key element in the preferential path of moisture distribution within the wall. Over time, their crystallization and expansion put pressure on the materials, resulting in structural damage [23,25].

The use of unilateral NMR sensors to map the distribution of moisture in the fresco has been applied to investigate the wall paintings of Brancacci's chapel, painted by Masolino, Masaccio and Filippo Lippi between 1425–1485. The investigation became necessary to understand the moisture distribution of the wall near the surface in relation to the environmental parameters at seasonal intervals.

Figure 5b shows the distribution maps obtained in two different seasons of the year by unilateral NMR at a depth of 1 mm on the left pillar of Brancacci Chapel, decorated with *Cacciata dei Progenitori dall'Eden* by Masaccio. The moisture distribution map derived from NMR data processing in the “Cacciata” scene was recorded in November 2022 and was suitably calibrated, see Figure 5b left, showing a moisture content (MC) in this area of the chapel to fall within the 0–6% range. Specifically, in the most humid region, an MC value of about 6% was found.

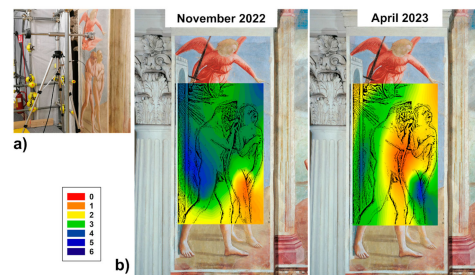


Figure 5. (a) Unilateral NMR instruments during the acquisition of a spin echo signal on the left pillar of Brancacci's Chapel decorated with the “Cacciata” scene; (b) Humidity maps recorded by NMR at a depth of 1 mm from the surface in November 2022 (left) and in April 2023 (right), respectively. The legend provides the humidity content range (%) obtained by calibrating the NMR signal.

A second monitoring campaign, conducted in April 2023 (see Figure 5b right), indicated a decrease in moisture distribution, with the MC values reduced from 4–5 to 3–1%.

2.2. NMR Stratigraphy for Paintings

One of the most recent applications of unilateral NMR sensors has been the characterization of material stratigraphy. Unilateral NMR allows for ^1H NMR signal amplitude encoding as a function of the scanned depth [5,7], providing information on the structure and thickness of the hydrogen-rich layers. This type of non-invasive investigation can be of great help in the conservation of paintings. Paintings are complex multilayer systems of organic and inorganic materials. Several factors can influence the degradation of paintings, such as environmental conditions, past restoration work and, finally, the type of painting technique and artistic materials used over the centuries. Two major challenges must be overcome to preserve the integrity of the object. First, during studies, a non-destructive method is required with minimal, or preferably no collection of samples to ensure its preservation and prevention of its degradation during studies. Secondly, the objects studied are often too precious and immovable, so the impossibility of bringing them to a laboratory leaves a study in situ as the only option. Unilateral NMR can provide information about the artist's work practices and techniques, and most importantly, contribute to the selection of proper and adequate conservation and restoration procedures.

In the field of paintings, two recent cases of application of stratigraphy NMR were here reported. In the first case, unilateral NMR was applied to evaluate the overlap of the pictorial layers in three paintings by Giuseppe Capogrossi, providing insights into the artist's technique. Secondly, unilateral NMR was applied to a painting by Alberto Burri to monitor its state of conservation and evaluate a previous restoration work, specifically, examining the adhesion of the original canvas to the new canvas applied on the back. This restoration had been carried out to strengthen the support of the pictorial film and to restore its initial tension.

Three paintings by Giuseppe Capogrossi were analyzed by unilateral NMR, called Surface 538, Surface 207 and Surface 553. Studies and restoration of his paintings have shown that he often reused the verses of the paintings or made changes to the works even after time. It is a well-known fact that sometimes Giuseppe Capogrossi has retouched the Surfaces exhibited in the room dedicated to him at the National Gallery of Modern and Contemporary Art in Rome.

As part of a project of conservation and restoration of the three paintings, the use of non-invasive NMR analysis allowed us to shed light on possible re-paintings and rethinking by the artist.

For each painting, areas with different colors were analyzed to assess the overlap of the layers. All the areas analyzed have the size of $2.5 \times 2.5 \text{ cm}^2$, and a micrometric thickness of about $20 \text{ }\mu\text{m}$. The profiles were executed by analyzing the entire thickness of the painting of about 1.5 mm with a step of about $50 \text{ }\mu\text{m}$.

In the painting Surface 538, three types of black—matt black, glossy black, and repainted black—can be observed. Figure 6a shows the NMR stratigraphies obtained on the areas painted in black. The opaque black areas, N1 and N2, consist of a thickness of about 0.4 mm . The glossy black areas, NL, and repainted black areas, Nr, instead show an increase in thickness due to the presence of several layers of painting. In particular, the thickest pictorial layer can be observed on the repainted black area, Nr, with a thickness almost double compared to the other areas analyzed and about 0.7 mm . The glossy area, NL, shows the overlap of two layers of different thickness: the most superficial layer relative to the glossy layer of about 0.2 mm and an underlying layer of about 0.4 mm , probably related to the matte black painting layer of the painting.

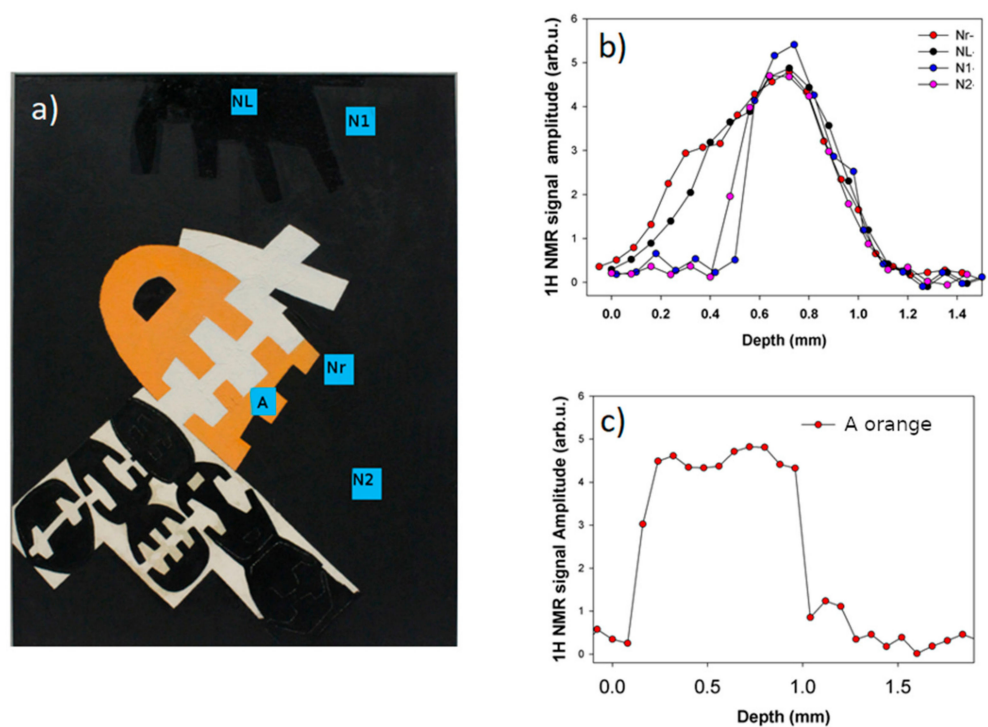


Figure 6. (a) Surface image 538, the letters indicate the measuring points. (b) ^1H NMR profiles obtained on the areas: NL—Glossy black area; Nr—Black area, repainted; N1—Matt black area without repainting; N2—Matt black area without repainting. (c) ^1H NMR profiles obtained on orange zone A.

Figure 6b shows the profile of the orange area, A. This point shows the profile of a painting layer thicker than the other areas, probably consisting of more than two layers. The total thickness is about 0.9 mm .

Figure 7 shows the image of surface 553 and the four areas analyzed with the NMR stratigraphy: 2 areas on white painting B1 and B2, an area on black painting N, and an area on red painting, R.

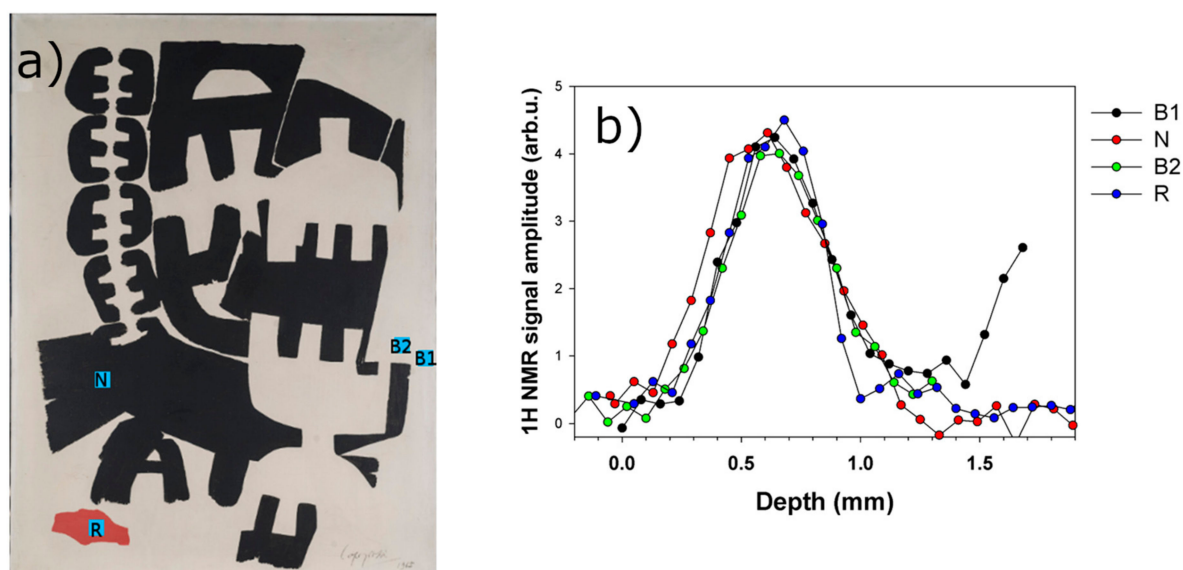


Figure 7. (a) image of painting 553; (b) profiles ^1H NMR on painting 553, obtained on the areas: B1—white on the frame, B2—white; and R—red.

The profiles show a pictorial layer with a thickness of about 0.6 mm in all areas analyzed. The area painted in black, N, shows a slight increase in thickness of about 0.1 mm. In the profile acquired on the white area at the frame, area B1, it is possible to observe at a depth of about 1.5 mm the signal of the hydrogen content of the wooden axis positioned below the canvas and which constitutes the frame of the painting. This data confirms that the thickness of the painting, including the canvas is about 1.2 mm.

The area under the frame, B1, does not show a thickness less than the yellowed area, B2. It is assumed that the yellowing is not due to the degradation of a layer above (paint type) that consequently should have increased the thickness of the painting, but to other types of degradation concerning the painting film.

For the painting surface 207, shown in Figure 8a, three colored areas were analyzed, C—celestial area; V—green area; B—white area; and two black areas Nv—opaque black area superimposed on green area; Nb—opaque black area, which are assumed to have been overwritten on white area blue, green and white.

Figure 8b shows the profiles obtained in the green, blue, and white areas. The areas analyzed show the pictorial layer with a thickness of about 0.6 mm.

Figure 8c,d show the comparisons of the ^1H NMR profiles obtained on the colored areas and on the black areas above. Both black areas analyzed show the presence of two layers of paint, the surface black of about 0.4 mm, and the underlying of about 0.6 mm relative to the colored area.

In conclusion, the measurements with unilateral NMR sensors allowed us to evaluate the thickness of the pictorial layers in different areas of the three paintings made by Capogrossi. It has been possible to obtain information on the thickness of the various layers over put and of the repainting of both the glossy layers and those affected by the rethinking, such as the white area repainted in black in the Surface 538.

The second case of application of the unilateral NMR sensors for studying painting stratigraphy is that of the artwork *Catrame* by Alberto Burri, characterized by using a material conglomerate not adhering to the support. This fragility, also from the point of view of conservation, made necessary in 1970 a significant restoration work. The intervention consisted of the replacement of the frame, the adhesion of the original canvas to a new

canvas applied on the back to strengthen the support of the pictorial film, and the leveling of the material conglomerates, involving a radical change of the painting.

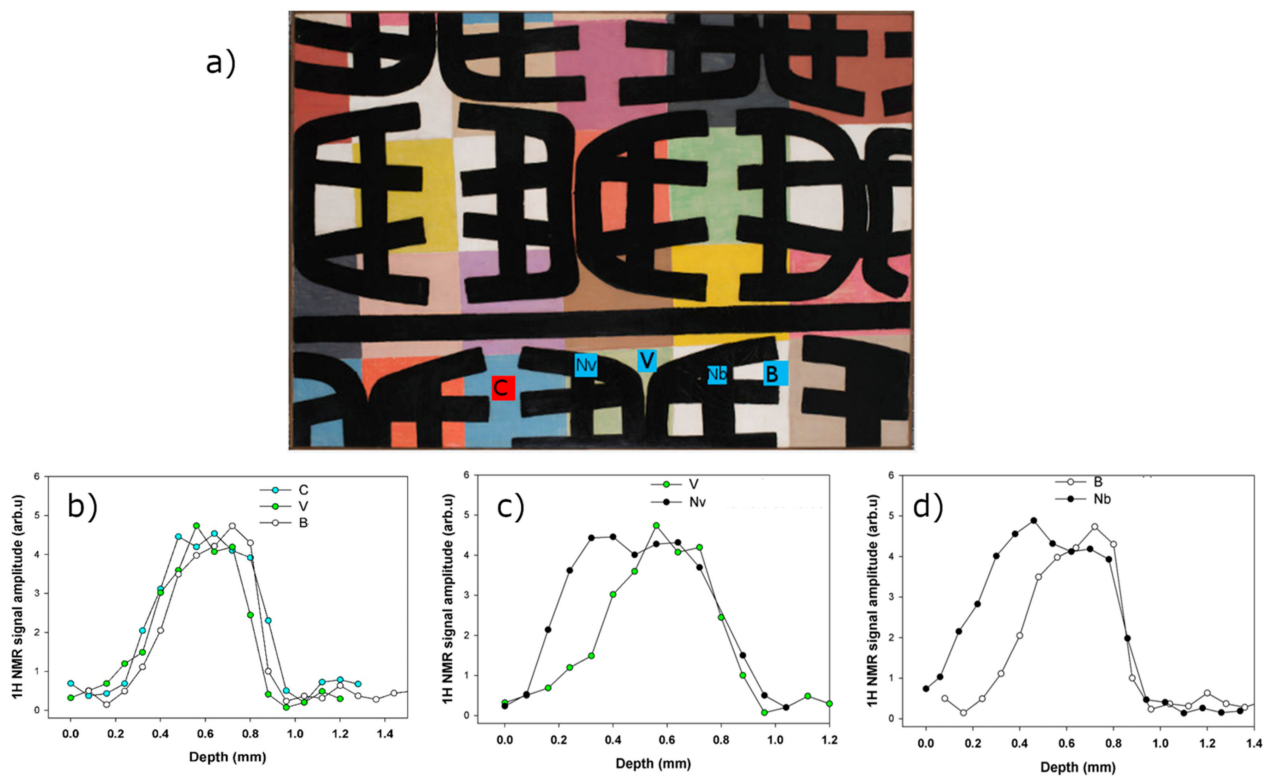


Figure 8. (a) Image of painting 207 with the areas analyzed with the NMR stratigraphy; (b) ^1H NMR profiles obtained on the C-celestial area areas; V green area; B white area; (c) comparisons of the ^1H NMR profiles obtained on the green area and on the opaque black area superimposed on the green area; (d) comparisons of the ^1H NMR profiles obtained on the white area and on the opaque black area superimposed on the white area, Nb.

The investigations carried out with unilateral NMR sensors on the painting *Catrame* by Alberto Burri, are placed within a diagnostic project that has as its objective the characterization of the constituent materials, the monitoring of the state of conservation of the painting and the evaluation of the adhesion of the new canvas on the original canvas before the next planned restoration work.

The stratigraphic profiles acquired with NMR have shown a high variability from area to area, due to the different pictorial execution of Burri, the different materials used, and the state of conservation. In this preliminary investigation of the painting, three types of statistical profiles have been identified, characterized by different total thicknesses: stratigraphic profile thickness less than 3 mm (point 6); stratigraphic profile thickness of about 3 mm (point 16); and lastly, the thickness of the stratigraphic profile greater than 3 mm (maximum value found 4 mm). Figure 9 shows three areas analyzed with different NMR stratigraphic thicknesses.

The profile was acquired by scanning the painting from the surface up to 5000 μm . The spatial range of acquisition has been modulated according to the type of area to be characterized, in the areas of the painting with greater pictorial inhomogeneity and in the presence of thick layers of painting, the profile was acquired for greater depth also making measurements from the back of the painting. The NMR profiles were then processed through a smoothing, reconstruction, and repositioning of the stratigraphies, considering the canvas support as the starting point (depth at 0 mm) while the end point (depth at 3–4 mm) the pictorial layer of the painting.

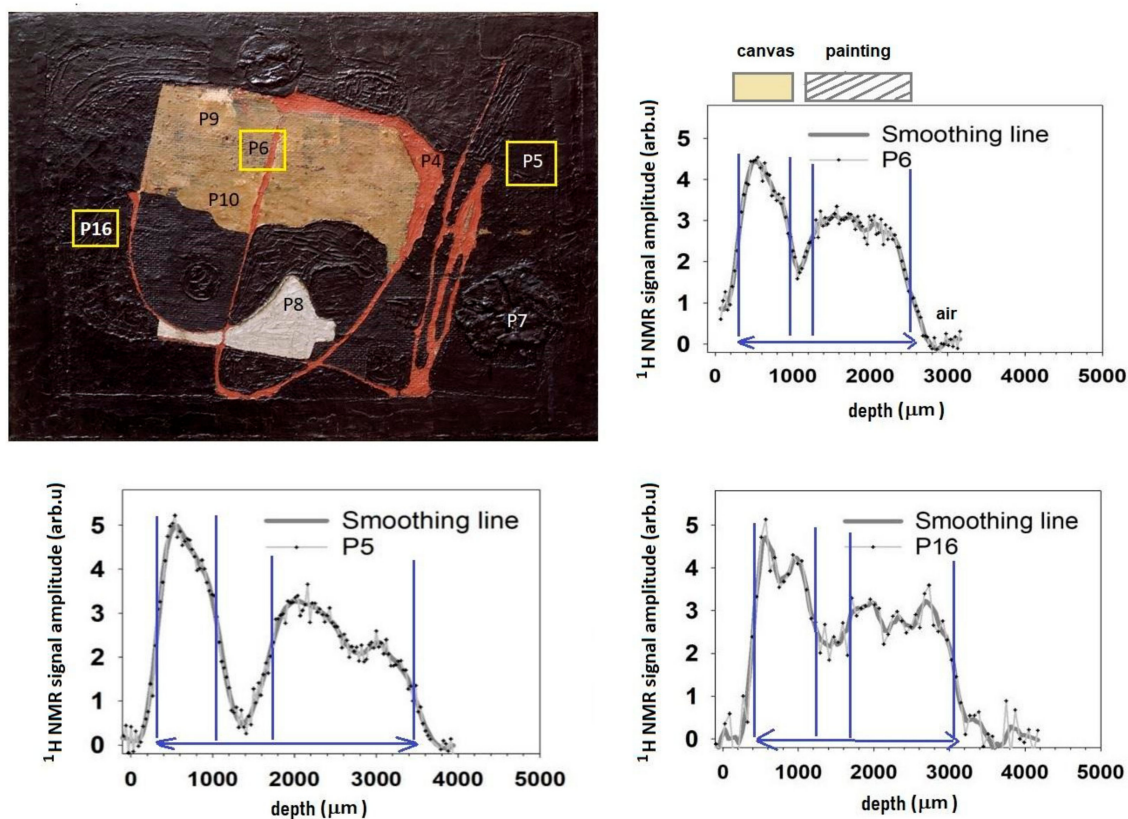


Figure 9. Top left shows an image of painting Catrame with the areas analyzed with the NMR stratigraphy is shown. The other graphs show the ^1H NMR profile of points P6, P16, and P5. In abscissa is shown the thickness/depth (depth) of scanning expressed in micrometers (μm), in ordinate is reported the signal NMR (arbitrary units) indicating the hydrogen content of the different layers constituting the painting. Above is a graphic diagram that suggests the possible correlation between the stratigraphy of the painting and the stratigraphic profile NMR.

The area analyzed in point 5 shows a wide stratigraphic profile that exceeds even 4 mm. In the above area is also visible a loss of NMR signal between the peak relative to the support (depth at about 0 mm) and the subsequent peak with a signal intensity, attributable to the following preparatory or pictorial layers. This lack of signal can be traced back to several causes, including the presence of detachments between the canvas and the original canvas, or the presence of mineral-charged grouting containing a low content of hydrogen, or finally the presence of original preparatory or pictorial layers made of materials with a low content of hydrogen (preparation with earth or limestone pigments).

To confirm and obtain a complete attribution of the signals of the stratigraphic profile, NMR is fundamental to the collection of information on the materials and methods used in previous restorations.

2.3. Unilateral NMR for Evaluating Degradation Processes: Study of Porosity in Lapidaceous Materials

The study of natural and artificial lapideous materials is a significant area of research within the field of cultural heritage preservation. Lapidaceous materials are essential components of historic structures, artifacts, and monuments, and understanding their properties and behavior over time is critical for their conservation and preservation for future generations [34,35]. From the macro-scale viewpoint, the issue is to maintain the structural integrity of the monument or manufacts as a whole. On the micro scale, the focus is on understanding the properties and behavior of individual materials. One of the key concerns in this research is the investigation of aspects related to the modification of the pore structure.

Porosity is a fundamental aspect to be evaluated, as it affects many degradation processes in lapideous materials. By studying such a parameter, it is, therefore, better understood how alteration phenomena occur, providing useful information for the conservation and preservation of historical–cultural heritage and architectural structures. It is often observed that analogous materials from a chemical and mineralogical perspective can undergo different alterations due to variations in their structural and textural characteristics, porosity, and all related parameters.

In the rigorous terms of physics, porosity is defined as: *“the ratio between the volume of voids, both interconnected and non-interconnected, present in a portion of material and the total, geometric volume of that portion”*. The general definition rightly mentions both communicating and non-communicating pores; in the specific context of degradation issues, non-communicating pores can instead be neglected, as alteration processes occur solely based on the movement of fluids, particularly water. Fundamental parameters, such as the amount of absorbed fluids, the rate of imbibition, and evaporation are intricately tied to porosity. These parameters provide insights into how textural and porosimetric characteristics govern the timing and modes of fluid circulation within the material. Notably, simpler methodologies, such as examining capillary imbibition curves or conducting total immersion and subsequent desorption tests—whether involving different materials or the same materials after artificial aging—offer valuable insights into these processes. Nevertheless, for a comprehensive understanding of fluid dynamics within the material, it is essential to measure the dimensional distribution of porosity, transcending beyond merely the global porosity value.

There are several analytical methodologies used to study porosity and its dimensional distribution in stone, each with its own advantages and limitations. One commonly used technique is mercury intrusion porosimetry (MIP), which involves forcing mercury into the pores of a stone sample under controlled conditions and measuring the pressure required to do so. This method allows for the quantification of the size, distribution, and volume of pores in a stone sample. Other methods include scanning electron microscopy (SEM), which can provide high-resolution images of the internal structure of a stone sample, and X-ray computed tomography (CT), which can produce 3D images of a sample’s internal structure and porosity. Another technique is nuclear magnetic resonance (NMR) spectroscopy, which provides information on the chemical and physical properties of the materials in a sample, including pore size and distribution. Nuclear magnetic resonance (NMR) is considered today an indispensable tool for the study of porous media in many research and industrial areas, such as in sedimentary rocks in the oil industry [36,37], soil research [38], or cement pastes [39]. However, conducting examinations of cultural heritage without causing damage requires non-invasive and non-destructive techniques. Unfortunately, there are only a limited number of non-invasive techniques available for the in situ evaluation of stone porosity, which makes this research challenging. Among these methods, unilateral NMR stands out as the only technique potentially applicable in the field for obtaining high-resolution images of pore size and distribution, dropping the need for invasive sampling or laboratory analysis on precious materials of interest in cultural heritage.

The NMR methods to probe porous media are based on the measurement of relaxation times and diffusion coefficients of water inside the porous matrix [40,41]. In fact, the relaxation times of fluids confined in porous media are strictly related to the geometry of the structure, as water in small pores relaxes rapidly, whereas water in large pores relaxes more slowly. The presence of relaxation sinks at the surface of pore grains and the inhomogeneity of pore dimensions cause multiexponential decay of the magnetization and a reduction in relaxation times. In the literature, numerous experiments on water-saturated rocks have compared relaxation–time distributions to pore–size distributions obtained by other techniques such as Mercury Intrusion Porosimetry (MIP) [42,43]. Both techniques can offer similar results in most porous materials, although NMR measures the size of pore bodies, whereas MIP measures the size of the pore throats. However, if there is a reasonably consistent factor between the pore throat and the body, then the relaxation-time distribution

may be similar to the pore-size distribution determined by MIP [44]. Because the relaxation times of confined water in porous media depends on pores size, a multi-exponential decay of the magnetization with echo time is expected. Commonly, several algorithms based on an inverse Laplace transformation are applied to the decay for obtaining a distribution of relaxation times [45]. In this representation, peak maxima are the most probable T_2 values and peak areas are the populations of each component. In addition to providing information on the porosity of building materials, unilateral NMR can also be used to assess other key physical properties, such as water content and diffusion rates.

Nevertheless, the limited resolution of portable NMR instruments may not be useful to detect small or narrow pores, which significantly influence the physical properties of a stone. This limitation poses a risk of underestimating porosity. Therefore, a comprehensive material characterization, employing various methodologies, including destructive ones, remains the preferred approach.

In this paper, Sabucina stones were analyzed by applying unilateral NMR to evaluate the effect of artificial mechanical degradations on the porosity distribution.

Sabucina stones have been a popular building material in Sicily for centuries, with ancient quarries supplying the material for many locally significant architectural structures and sculptures. This yellow bioclastic calcarenite, known geologically as Capodarso Calcarenites—Enna Fm., is a Pliocene formation with excellent physical and mechanical properties, as well as aesthetic features that make it a popular replacement stone for Baroque monuments in the Noto Valley, which are included in the UNESCO Heritage List.

Sabucina stone can be classified as a biosparite. Its allochems consist of small bioclast fragments, while its orthochems are predominantly made up of spathic calcite, with a small amount of micrite with an uneven distribution (the texture varies between grainstone and packstone). The siliciclastic component is due to sub-rounded quartz grains (2–3 vol%; ~100 μm). The stone's porosity is interparticle, moldic, and vuggy [46], comprising 20–30% of its volume. Referring to behavior of stone against water by capillarity and total immersion, standard tests [47,48] give back values of 0.02 g/cm^2 and 11.07%, respectively, without variations related to directions (isotropic texture). Accelerating aging test [49] were carried out on samples, providing an average of –11.09% mass loss after 15 weathering cycles, with a “salt controlled” behavior (positive mass variation) until the fourth-five cycles and a “weathered controlled” (negative mass variation) from the sixth one. The degradation process mainly occurs by disintegrating the samples from the edges, resulting in the formation of white patinas associated with chromatic changes, granular disintegration, and powdering. Porosity and pore size distribution investigated by mercury intrusion porosimetry tests (MIP) [50] highlight a total accessible porosity of 26.86% and a total pore volume of 0.1356 g/cm^3 . Referring to pore size distribution, an average pore radius of 0.1442 μm and a mode peak at 8.5567 μm have been obtained.

In Figure 10, results obtained by applying NMR to the Sabucina sample for analyzing porosity distribution before and after degradation are shown. The decay constant T_2 is proportional to the pore size, with smaller pores characterized by shorter relaxation times compared to those measured in larger pores. In the Sabucina untreated sample, five components of T_2 were observed, with a proton density centered in the medium pores size (see Table 1). After the aging test, results indicated an increase in the longest component of T_2 with the number of weathering cycles, reaching a normalized proton density of approximately 40% of the total pore size population. This shift to larger values of T_2 indicates an enlargement of pore sizes due to mechanical aging.

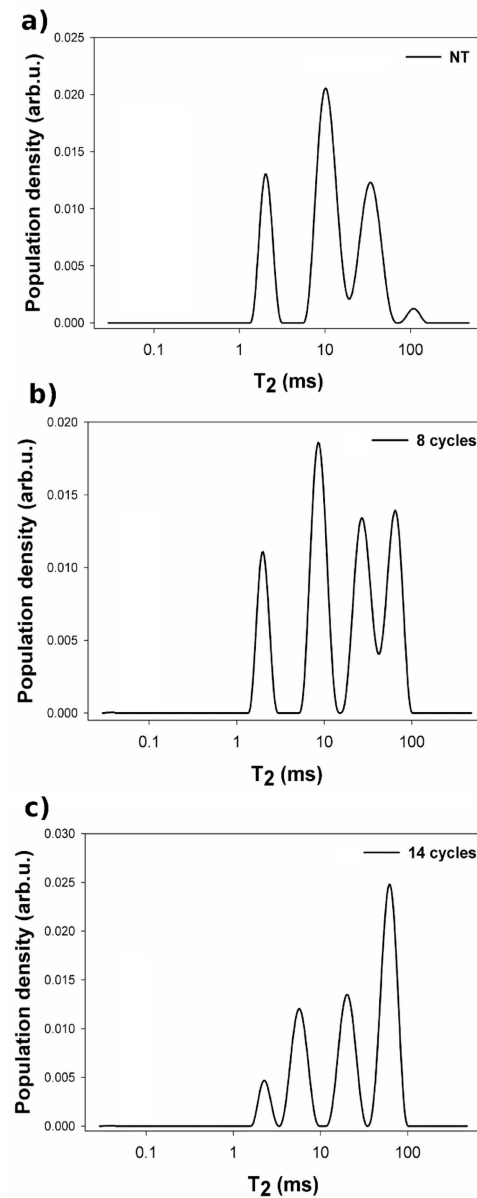


Figure 10. Comparison of distributions of T_2 in the Sabucina Stone before and after artificial aging. (a) untreated sample (NT); (b) sample aged for 8 cycles aging sample; and (c) sample aged for 14 cycles. The distribution of T_2 was obtained by averaging and fitting the signal of the transverse component of the magnetization acquired at depths of 1000, 700, and 400 μm from the surface of the sample.

Table 1. Values of T_2 and their proton densities, expressed as weight (W) and normalized to 100, measured in the untreated sample, and after aging with 8 and 14 cycles. The reported values were calculated by averaging three distributions acquired at 1000, 700 and 400 μm .

| Sample | W_A (%) | T_{2A} (ms) | W_B (%) | T_{2B} (ms) | W_C (%) | T_{2C} (ms) | W_D (%) | T_{2D} (ms) | W_E (%) | T_{2E} (ms) |
|------------------|-----------|----------------|-----------|---------------|-----------|---------------|-----------|---------------|-----------|---------------|
| Untreated sample | 17 | 0.1 ± 0.01 | 16 | 2.1 ± 0.3 | 40 | 10 ± 2 | 25 | 35 ± 5 | 2 | 113 ± 16 |
| 8 cycles | 10 | 0.1 ± 0.01 | 14 | 2.1 ± 0.3 | 30 | 8 ± 2 | 25 | 27 ± 5 | 21 | 68 ± 16 |
| 14 cycles | 16 | 0.1 ± 0.01 | 5 | 2.3 ± 0.3 | 18 | 6 ± 2 | 18 | 21 ± 5 | 40 | 62 ± 16 |

As reported, the distribution obtained by applying portable NMR can help conservators in evaluating the effects of the degradation phenomena on the porosity by comparing

the results before and after the aging test. However, it is important to note that, even though T_2 values can potentially be used to estimate pores size, the data obtained through such processing cannot be considered as the effective dimensions of the pores. This is because, with portable NMR, the signal was acquired under an inhomogeneous magnetic field. In a homogeneous field, the transverse relaxation rates $\left(\frac{1}{T_2}\right)$ in saturated porous media may be written as follows:

$$\frac{1}{T_2} = \frac{1}{T_{2b}} + \rho_2 \frac{S}{V} \quad (4)$$

where T_{2b} are the bulk relaxation times, $\rho_2 \frac{S}{V}$ originates from the molecules in contact with the pore surface, ρ_2 is the surface relaxivity, and $\frac{S}{V}$ is the surface to volume ratio. Bulk contributions are often much smaller than those of surfaces and in many cases may be neglected. However, in the presence of a magnetic field gradient of strength G , attenuation due to molecular diffusion must be accounted for. The gradient may originate from variations in the magnetic susceptibility associated with pore geometry or from inhomogeneity in the applied magnetic field B_0 . Therefore, in strongly inhomogeneous polarization and RF fields such as the case of unilateral NMR, the transverse spin–spin relaxation rate also depends on the G strength:

$$\frac{1}{T_2} = \frac{1}{T_{2b}} + \rho_2 \frac{S}{V} + \frac{D(\gamma G t_E)^2}{12} \quad (5)$$

where D is the diffusion coefficient, γ is the gyromagnetic ratio of the nucleus observed, and t_E is the echo time. The effect of diffusion may be significantly reduced by employing a CPMG sequence with the shortest possible echo time to measure T_2 . In Figure 11, the okT_2 distributions of the Sabucina stone under homogeneous and inhomogeneous magnetic fields were compared. As expected, although the number of T_2 components is the same, a shortening of T_2 values can be observed.

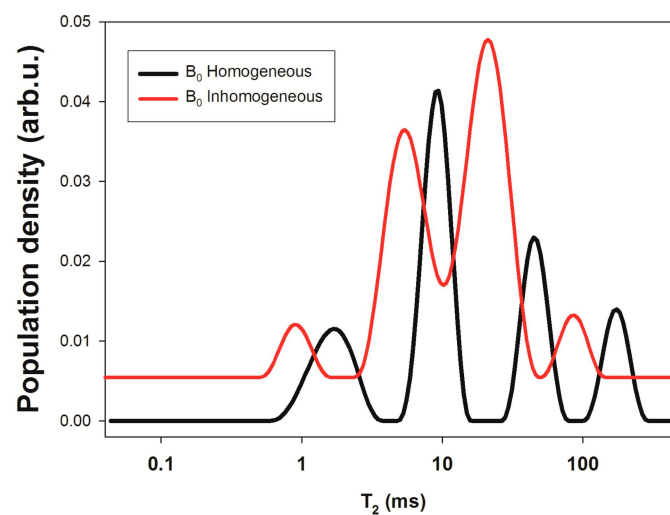


Figure 11. Distributions of T_2 obtained by acquiring the NMR signal (RF 20 MHz) under a homogeneous magnetic field (Minispec MQ-Bruker-sample dimension 10 mm) and an inhomogeneous magnetic field (portable NMR-Magritek).

3. Experimental Details

3.1. Moisture in Masonry

3.1.1. Church of San Nicola in Carcere

Measurements were performed in situ with a unilateral NMR instrument from Bruker Biospin, see Figure 1a, operating at 17 MHz, at a depth of 0.3 cm from the surface, fully disregarding the signal from the surface. The maximum echo signal corresponding to a $\pi/2$ pulse was obtained with a pulse width of 3 μ s. The dead time was 15 μ s. Measurements

were carried out in the lower part of the apse along a matrix of 50 points appropriately chosen to cover an area with a height of 120 cm and a width of about 1100 cm. Each measured point corresponded to an area of 10 cm², which is the area that the probe head detects.

3.1.2. Priscilla Catacombs

Measurements were performed in situ with a unilateral NMR instrument from Bruker Biospin, see Figure 1a, operating at 16 MHz, at a depth of 0.5 cm from the surface, fully disregarding the signal from the surface. The maximum echo signal corresponding to a $\pi/2$ pulse was obtained with a pulse width of 16 μ s. The dead time was 15 μ s. Measurements were carried out on an area of the Greek Chapel, on a matrix of 18 points. Each measured point corresponded to an area of 10 cm².

3.1.3. Brancacci Chapel

Measurements were performed in situ with a unilateral NMR instrument from Bruker Biospin, see Figure 1a, operating at 18 MHz, at a depth of 0.1 cm from the surface, fully disregarding the signal from the surface. The maximum echo signal corresponding to a $\pi/2$ pulse was obtained with a pulse width of 3 μ s. The dead time was 15 μ s. Measurements were carried out on the left pillar of the Brancacci Chapel, decorated with the Cacciata dei Progenitori dall'Eden by Masaccio on a matrix of 13 points. Each measured point corresponded to an area of 10 cm².

3.2. Paintings

3.2.1. Capogrossi Paintings

¹H NMR stratigraphies were collected at 13.62 MHz with a unilateral NMR instrument by Magritek, see Figure 1b, interfaced with a Bruker Biospin electronic unit that can scan depths from 0 up to 1.0 cm. Experiments were carried out by repositioning the single-sided sensor in steps of 30 μ m to cover the desired spatial range, from the outermost surface of the painting to a depth of 0.15 cm; the number of scans was 256. The area of measurement was 2.5 \times 2.5 cm².

3.2.2. Burri Painting

¹H NMR stratigraphies were collected at 13.62 MHz with a unilateral NMR instrument by Magritek, see Figure 1b, interfaced with a Bruker Biospin electronic unit that can scan depths from 0 up to 1.0 cm. Experiments were carried out by repositioning the single-sided sensor in steps of 30 μ m to cover the desired spatial range, from the outermost surface of the painting to a depth of 0.5 cm; the number of scans was 1024. The area of measurement was 2.5 \times 2.5 cm².

3.3. Porosity in Lapidous Materials

Measurements were carried out at 13.62 MHz with a unilateral NMR instrument by Magritek, see Figure 1b, interfaced with a Bruker Biospin electronic unit that can scan depths from 0 up to 1.0 cm. Transverse relaxation times T_2 were measured using the CPMG pulse sequence, with 4.096 echoes were recorded with an echo time of 58.5 μ s. Because the field generated by unilateral NMR is inhomogeneous, an effective transverse relaxation times $T_{2\text{eff}}$ is obtained and it may be shorter than that measured in a homogeneous field. The shortening of the transverse relaxation time can be minimized by using an echo spacing as short as possible.

TD-NMR experiments were conducted on a Minispec mq 20 pulsed NMR spectrometer by Bruker, with an operating at a frequency of 20 MHz for protons (magnetic field strength: 0.47 T). The NMR spectrometer was equipped with an external thermostat (HAAKE K20) to maintain the desired temperature conditions. The measurements were carried out at 25 °C (± 1 °C), and before NMR measurements, the tube was placed into the NMR probe for approximately ca. 15 min for thermal equilibration. Transverse relaxation measurements

were performed using the Carr–Purcell–Meiboom–Gill (CPMG) sequence with a pulse spacing of 0.04 ms, between two following 180° pulses, of 0.04 ms; about 8000 echoes were recorded. Measurements with the Minispec were performed to evaluate the T_2 distribution under a homogeneous magnetic field.

4. Conclusions

Recent developments of the portable NMR instrument have allowed for the increasing use of the NMR methodology in the cultural heritage field. In this paper, some recent applications of portable NMR sensors are shown.

The non-invasive evaluation of humidity in the masonry by portable NMR is one of the first applications of this portable technique to wall paintings and masonries. Three different cases of humidity in masonries have been reported. Using probes at different depths of penetration, unilateral NMR is able to investigate different regions of the masonry affected by different moisture problems. For capillary rise and percolating humidity, probes at 3 mm and 5 mm depth are used, disregarding the contribution of the surface, while for the condensation humidity, probes at 1 mm depth are very useful to evaluate the surface exchange of moisture of wall with the environment. Moreover, with a suitable calibration procedure, unilateral NMR is still the only one non-invasive technique to evaluate a quantitative distribution of moisture content in the first millimeters of masonries.

Another application is the non-invasive NMR stratigraphy of paintings. Unilateral NMR allows for ^1H NMR signal amplitude encoding as a function of the scanned depth, providing information on the structure and thickness of the hydrogen-rich layers. The study on three paintings by Capogrossi were showed. The use of non-invasive NMR analysis allowed us to shed light on possible re-paintings and rethinking by the artist. Secondly, the portable NMR was used for monitoring the state of conservation of the painting *Catrame* by Burri and for evaluating a previous restoration work, specifically, examining the adhesion of the original canvas to the new canvas applied on the back.

Finally, an application of unilateral NMR on lapideous materials is shown for evaluating degradation processes and studying the porosity of stones. Porosity is a fundamental aspect to be evaluated, as it affects many degradation processes in lapideous materials. The study of this parameter allows us to better understand how alteration phenomena occur, providing useful information for the conservation and preservation of historical-cultural heritage and architectural structures. In this paper, Sabucina stone, a popular building material in Sicily, was analyzed by unilateral NMR to evaluate the effect of artificial mechanical degradations on the porosity distribution. After the aging test, NMR parameter T_2 measurements indicates an increase in the size of pores caused by mechanical aging. Thus, unilateral NMR stands out as the only technique potentially applicable in the field for obtaining high-resolution images of pore size and distribution, dropping the need for invasive sampling or laboratory analysis on precious materials of interest in cultural heritage.

Author Contributions: V.D.T.: collaboration on data curation, review and editing; N.P.: conceptualization, data curation, writing, review and editing. All authors have read and agreed to the published version of the manuscript.

Funding: This research was funded by Regione Lazio (Italy), ADAMO project “Analysis, Diagnostic and Monitoring Technologies for the conservation and restoration of cultural heritage”, Project ADAMO n. B86C18001220002 of the Excellence Centre at the Lazio Technological District for cultural heritage (2018–2020) and REMEDIA project “Research and diagnostics of methods to contrast the deterioration caused by humidity in Cultural Heritage” A0375-2020-36497 (2021–2024). Capogrossi’s painting study is part of a research project supported by IPERION CH.IT (laboratory MOLAB and FIXLAB), infrastructure of E-HIRS (European Research Infrastructure for Heritage Science).

Data Availability Statement: The original contributions presented in the study are included in the article, further inquiries can be directed to the corresponding author.

Acknowledgments: The authors wish to acknowledge Paola Carnazza of the National Gallery of Modern Art (GNAM) in Rome. Capogrossi's painting study is part of a research project supported by IPERION CH.IT (laboratory MOLAB and FIXLAB), infrastructure of E-HIRS (European Research Infrastructure for Heritage Science). The authors thanks to Cristiano Riminesi of CNR ISPC, Area della Ricerca di Firenze (Italy) and Alberto Felici of SABAP-FI (Italy). Brancacci Chapel is part of a research project "Analisi e monitoraggio per il restauro degli affreschi della Cappella Brancacci nella basilica di Santa Maria del Carmine a Firenze" by Comune di Firenze, CNR-ISPC, SABAP-FI.

Conflicts of Interest: The authors declare no conflicts of interest.

References

1. Pozzi, F.; Rizzo, A.; Basso, E.; Angelin, E.M.; de Sá, S.F.; Cucci, C.; Picollo, M. Portable Spectroscopy for Cultural Heritage. In *Portable Spectroscopy and Spectrometry*; Crocombe, R., Leary, P., Kammrath, B., Eds.; John Wiley & Sons, Inc.: Hoboken, NJ, USA, 2021. [[CrossRef](#)]
2. Valentini, F.; Calcaterra, A.; Antonaroli, S.; Talamo, M. Smart Portable Devices Suitable for Cultural Heritage: A Review. *Sensors* **2018**, *18*, 2434. [[CrossRef](#)] [[PubMed](#)]
3. Eidmann, G.; Savelsberg, R.; Blümer, P.; Blümich, B. The NMR-MOUSE, a mobile universal surface explorer. *J. Magn. Reson. A* **1996**, *122*, 104–109. [[CrossRef](#)]
4. Perlo, J.; Demas, V.; Casanova, F.; Meriles, C.A.; Reimer, J.; Pines, A.; Blümich, B. High resolution NMR spectroscopy with a portable single-sided sensor. *Science* **2005**, *308*, 127. [[CrossRef](#)] [[PubMed](#)]
5. Perlo, J.; Casanova, F.; Blümich, B. Profiles with microscopic resolution by single-sided NMR. *J. Magn. Reson.* **2005**, *176*, 64–70. [[CrossRef](#)] [[PubMed](#)]
6. Proietti, N.; Capitani, D.; Lamanna, R.; Presciutti, F.; Rossi, E.; Segre, A.L. Fresco Paintings studied by unilateral NMR. *J. Magn. Reson.* **2005**, *177*, 111–117. [[CrossRef](#)] [[PubMed](#)]
7. Presciutti, F.; Perlo, J.; Casanova, F.; Glöggler, S.; Miliani, C.; Blümich, B.; Brunetti, B.G.; Sgamellotti, A. Noninvasive nuclear magnetic resonance profiling of painting layers. *Appl. Phys. Lett.* **2008**, *93*, 033505. [[CrossRef](#)]
8. Casanova, F.; Perlo, J. NMR in Inhomogeneous Fields. In *Single-Sided NMR*; Springer: Berlin, Germany, 2011; pp. 11–55.
9. Blümich, B.; Casanova, F.; Perlo, J.; Presciutti, F.; Anselmi, C.; Doherty, B. Noninvasive Testing of Art and Cultural Heritage by Mobile NMR. *Acc. Chem. Res.* **2010**, *43*, 761–770. [[CrossRef](#)] [[PubMed](#)]
10. Del Federico, E.; Centeno, S.A.; Kehlet, C.; Currier, P.; Stockman, D.; Jerschow, A. Unilateral NMR applied to the conservation of works of art. *Anal. Bioanal. Chem.* **2010**, *396*, 213–222. [[CrossRef](#)] [[PubMed](#)]
11. Proietti, N.; Presciutti, F.; Di Tullio, V.; Doherty, B.; Marinelli, A.M.; Provinciali, B.; Macchioni, N.; Capitani, D.; Miliani, C. Unilateral NMR, ¹³C CPMAS NMR spectroscopy and micro-analytical techniques for studying the materials and state of conservation of an ancient Egyptian wooden sarcophagus. *Anal. Bioanal. Chem.* **2011**, *399*, 3117–3131. [[CrossRef](#)] [[PubMed](#)]
12. Rühli, F.J.; Böni, T.; Perlo, J.; Casanova, F.; Baias, M.; Egarter, E.; Blümich, B. Non-invasive spatial tissue discrimination in ancient mummies and bones in situ by portable nuclear magnetic resonance. *J. Cult. Herit.* **2007**, *8*, 257–263. [[CrossRef](#)]
13. Di Tullio, V.; Capitani, D.; Presciutti, F.; Gentile, G.; Brunetti, B.G.; Proietti, N. Non-invasive NMR stratigraphy of a multi-layered artefact: An ancient detached mural painting. *Anal. Bioanal. Chem.* **2013**, *405*, 8669–8675. [[CrossRef](#)] [[PubMed](#)]
14. Brizi, L.; Bortolotti, V.; Marmotti, G.; Camaiti, M. Identification of complex structures of paintings on canvas by NMR: Correlation between NMR profile and stratigraphy. *Magn Reson Chem.* **2020**, *58*, 889–901. [[CrossRef](#)]
15. Keine, S.; Holthausen, R.S.; Raupach, M. Single-sided NMR as a non-destructive method for quality evaluation of hydrophobic treatments on natural stones. *J. Cult. Herit.* **2019**, *36*, 128–134. [[CrossRef](#)]
16. Di Tullio, V.; Scitutto, G.; Proietti, N.; Prati, S.; Mazzeo, R.; Colombo, C.; Cantisani, E.; Romè, V.; Rigaglia, D.; Capitani, D. ¹H NMR depth profiles combined with portable and micro-analytical techniques for evaluating cleaning methods and identifying original, non-original, and degraded materials of a 16th century Italian wall painting. *Microchem. J.* **2018**, *141*, 40–50. [[CrossRef](#)]
17. Hürlimann, M.D.; Venkataramanan, L. Quantitative measurement of two dimensional distribution functions of diffusion and relaxation in grossly inhomogeneous fields. *J. Magn. Reson.* **2002**, *157*, 31–42. [[CrossRef](#)] [[PubMed](#)]
18. Awad, W.M.; Baias, M. How mobile NMR can help with the conservation of paintings. *Magn Reson Chem.* **2020**, *58*, 792–797. [[CrossRef](#)] [[PubMed](#)]
19. Franzoni, E. Rising damp removal from historical masonries: A still open challenge. *Constr. Build. Mater.* **2014**, *54*, 123–136. [[CrossRef](#)]
20. Rosina, E. When and how reducing moisture content for the conservation of historic building. A problem solving view or monitoring approach? *J. Cult. Herit.* **2018**, *31*, S82–S88.
21. Killip, I.; Cheetham, D. The prevention of rain penetration through external walls and joints by means of pressure equalization. *Build. Environ.* **1984**, *19*, 81–91. [[CrossRef](#)]
22. Blocken, B.; Carmeliet, J. Overview of three state-of-the-art wind-driven rain assessment models and comparison based on model theory. *Build. Environ.* **2010**, *45*, 691–703. [[CrossRef](#)]
23. López-Arce, P.; Doehne, E.; Greenshields, J.; Benavente, D.; Young, D. Treatment of rising damp and salt decay: The historic masonry buildings of Adelaide, South Australia. *Mater. Struct.* **2008**, *42*, 827–848.

24. Sandrolini, F.; Franzoni, E.; Vio, E.; Lonardoni, S. Challenging transient flooding effects on dampness in brick masonry in Venice by a new technique: The narthex in St. Marco Basilica. In *Flooding and Environmental Challenges for Venice and Its Lagoon: State of Knowledge*. In Proceedings of the International Conference Flooding and Environmental Challenges for Venice and Its Lagoon, Cambridge, UK, 14–17 September 2003; Cambridge University Press: Cambridge, UK, 2005; p. 181.
25. Di Tullio, V.; Proietti, N.; Gentile, G.; Giani, E.; Poggi, D.; Capitani, D. Unilateral NMR: A Noninvasive Tool for Monitoring In Situ the Effectiveness of Intervention to Reduce the Capillary Rise of Water in an Ancient Deteriorated Wall Painting. *Int. J. Spectrosc.* **2012**, *2012*, 494301. [[CrossRef](#)]
26. Sandrolini, F.; Franzoni, E. An operative protocol for reliable measurements of moisture in porous materials of ancient buildings. *Build. Environ.* **2006**, *41*, 1372–1380. [[CrossRef](#)]
27. Sansonetti, A.; Rosina, E.; Ludwig, N. Moisture damage. *Mater. Eval.* **2011**, *69*, 41–46.
28. Di Tullio, V.; Proietti, N.; Gobbino, M.; Capitani, D.; Olmi, R.; Priori, S.; Riminesi, C.; Giani, E. Non-destructive mapping of dampness and salts in degraded wall paintings in hypogeous buildings: The case of St. Clement at mass fresco in St. Clement Basilica, Rome. *Anal. Bioanal. Chem.* **2010**, *396*, 1885–1896. [[CrossRef](#)] [[PubMed](#)]
29. Proietti, N.; Capitani, D.; Cozzolino, S.; Valentini, M.; Pedemonte, E.; Princi, E.; Vicini, S.; Segre, A.L. In Situ and Frontal Polymerization for the Consolidation of Porous Stones: A Unilateral NMR and Magnetic Resonance Imaging Study. *J. Phys. Chem. B.* **2006**, *110*, 23719–23728. [[CrossRef](#)] [[PubMed](#)]
30. Lubelli, B.; Van Hees, R.; Bolhuis, J. Effectiveness of methods against rising damp in buildings: Results from the EMERISDA project. *J. Cult. Herit.* **2018**, *31*, S15–S22. [[CrossRef](#)]
31. I'Anson, S.; Hoff, W. Water movement in porous building materials-VIII. Effects of evaporative drying on height of capillary rise equilibrium in walls. *Build. Environ.* **1986**, *21*, 195–200.
32. Hall, C.; Hoff, W.D. Rising damp: Capillary rise dynamics in walls. *Proc. R. Soc. A Math. Phys. Eng. Sci.* **2007**, *463*, 1871–1884.
33. Proietti, N.; Calicchia, P.; Colao, F.; De Simone, S.; Di Tullio, V.; Luvidi, L.; Prestileo, F.; Romani, M.; Tati, A. Moisture Damage in Ancient Masonry: A Multidisciplinary Approach for In Situ Diagnostics. *Minerals* **2021**, *11*, 406. [[CrossRef](#)]
34. Siegesmund, S.; Weiss, T.; Vollbrecht, A. Natural stone, weathering phenomena, conservation strategies and case studies: Introduction. *Geol. Soc. Lond. Spec. Publ.* **2002**, *205*, 1–7. [[CrossRef](#)]
35. Doehne, E.; Price, C.A. *Stone Conservation: An Overview of Current Research*, 2nd ed.; Getty Conservation Institute: Los Angeles, CA, USA, 2010; p. 176.
36. Song, Y.-Q. Magnetic resonance of porous media (MRPM): A perspective. *J. Magn. Reson.* **2013**, *229*, 12. [[CrossRef](#)] [[PubMed](#)]
37. Kleinberg, R.L.; Kenyon, W.E.; Mitra, P.P. Mitra, Mechanism of NMR relaxation of fluids in rocks. *J. Magn. Reson. Ser. A* **1994**, *108*, 206–214. [[CrossRef](#)]
38. Stingaciu, L.R.; Pohlmeier, A.; Blümner, P.; Weihermüller, L.; van Dusschoten, D.; Stapf, S.; Vereecken, H. Characterization of unsaturated porous media by high-field and low-field NMR relaxometry. *Water Resour. Res.* **2009**, *45*, W08412. [[CrossRef](#)]
39. Monteilhet, L.; Korb, J.P.; Mitchell, J.; McDonald, P.J. Observation of exchange of micropore water in cement pastes by two-dimensional T₂-T₂ nuclear magnetic resonance relaxometry. *Phys. Rev. E Stat. Nonlinear Soft Matter Phys.* **2006**, *74*, 1. [[CrossRef](#)] [[PubMed](#)]
40. Chen, S.; Liaw, H.K.; Watson, A.T. Fluid saturation-dependent nuclear magnetic resonance spin-lattice relaxation in porous media and pore structure analysis. *J. Appl. Phys.* **1993**, *74*, 1473–1479. [[CrossRef](#)]
41. Watson, A.T.; Chang, C.T. Characterizing porous media with NMR methods. *Progr. Nucl. Magn. Reson. Spectrosc.* **1997**, *31*, 343–386. [[CrossRef](#)]
42. Zhang, Y.; Xu, S.; Gao, Y.; Guo, J.; Cao, Y.; Zhang, J. Correlation of chloride diffusion coefficient and microstructure parameters in concrete: A comparative analysis using NMR, MIP, and X-CT. *Front. Struct. Civ. Eng.* **2020**, *14*, 1509–1519. [[CrossRef](#)]
43. Zuena, M.; Tomasin, P.; Alberghina, M.F.; Longo, A.; Marrale, M.; Gallo, S.; Zendri, E. Comparison between mercury intrusion porosimetry and nuclear magnetic resonance relaxometry to study the pore size distribution of limestones treated with a new consolidation product. *Measurement* **2019**, *143*, 234–245. [[CrossRef](#)]
44. Dunn, K.J.; Bergman, D.J.; Latorraca, G.A. *Nuclear Magnetic Resonance Petrophysical and Logging Applications*; Pergamon: Oxford, UK, 2002.
45. Borgia, G.C.; Brown, R.J.S.; Fantazzini, P. Uniform-penalty inversion of multiexponential decay data. *J. Magn. Reson.* **1998**, *1321*, 65–77. [[CrossRef](#)]
46. Choquette, P.W.; Pray, L.C. Geologic Nomenclature and Classification of Porosity in Sedimentary Carbonates. *Am. Assoc. Pet. Geol. Bull.* **1970**, *54*, 207–250.
47. *NORMAL 11/88*; Natural Stones Test Methods: Determination of Water Absorption Coefficient by CNR-ICR. CNR-ICR: Rome, Italy, 2000.
48. *NORMAL 7/81*; Natural Stones Test Methods: Determination of Water Absorption by Total Immersion. CNR-ICR: Rome, Italy, 1981.
49. *EN 12370:2001*; Natural Stone Test Methods—Determination of Resistance to Salt Crystallization. European Standard: Brussels, Belgium, 2001.
50. Raneri, S.; Barone, G.; Mazzoleni, P.; Rabot, E. Visualization and quantification of weathering effects on capillary water uptake of natural building stones by using neutron imaging. *Appl. Phys. A* **2016**, *122*, 969. [[CrossRef](#)]

Disclaimer/Publisher's Note: The statements, opinions and data contained in all publications are solely those of the individual author(s) and contributor(s) and not of MDPI and/or the editor(s). MDPI and/or the editor(s) disclaim responsibility for any injury to people or property resulting from any ideas, methods, instructions or products referred to in the content.